International Journal of Computational and Experimental Science and ENgineering (IJCESEN)

Vol. 11-No.3 (2025) pp. 3979-3994
http://www.ijcesen.com

ISSN: 2149-9144

Research Article

Flexural Behavior of Steel-Precast Concrete Composite Girder Using UHPC Shear Pockets

Enas Sami Sabbar[1], Haider M. Al-Jelawy[2*]

[1]Civil Engineering Department, University of Al-Qadisiyah, Ad Diwaniyah, Iraq
Email: civil8@qu.edu.iq **- ORCID:** 0000-0002-5245-7850

[2]Roads and Transport Engineering Department, University of Al-Qadisiyah, Ad Diwaniyah, Iraq
* **Corresponding Author Email:** haider.aljelawy@qu.edu.iq **- ORCID**: 0000-0002-5246-7850

Article Info:

DOI: 10.22399/ijcesen.2254
Received : 03 March 2025
Accepted : 25 May 2025

Keywords :

Steel-UHPC Composite Beams
Shear Stud Clusters
Shear Pocket
Precast Concrete Deck Slab
Structural Behaviour
Strengthening

Abstract:

This paper presents an experimental investigation into the behavior of a composite concrete steel bridge girder under four point loads. Five RC specimens have been considered in the experimental tests with a UHPC haunch layer and variable number of shear pockets. One specimen has been represented by the specimens to be the reference specimen, while the other specimens tested as strengthened composite beams. Two variables have been considered in the experimental tests: the number of shear pockets and the alignment line of bolt studs (straight and zigzag lines). The deflection at the center of the beam, the first crack, the cracking load, and the crack pattern were studied. The test results show that it was determined that the ultimate load capacity of zigzag-line alignments for three shear pockets increased from the reference beams with 63.91%. Whereas, in comparison to reference specimens, ultimate load capacity for all beams increases by about 47% for 60%. In addition, no splitting cracks are observed in UHPC shear pockets, and no concrete crushing occurs on the surface of the UHPC slab at the failure of beam specimens. The UHPC and steel exhibit good composite action, and the flexural performance of steel-UHPC composite beams is significantly improved.

1. Introduction

Bridge decks are expected to endure numerous repeated vehicle loads in their service life. In recent years, numerous types of steel-concrete composite slabs have been developed and used on bridge decks. These materials produce a structural system that is both cost-effective and interesting by combining the compressive strength and rigidity of concrete with the strength of steel. At the beginning, the most popular composite beam form has been an I-steel profile that is connected to the concrete slab or a profiled steel-concrete composite slab. A composite beam is more common in contemporary constructions where steel beams are joined to the concrete slab using different kinds of shear connections so that the two function as a single unit [1]. In this case, the concrete slab is primarily subject to compressive pressures, while the steel beam is subjected to tensile stresses, thus utilising the beneficial characteristics of each material [2-4]. The shear strength at the steel–concrete interface is one of the most significant issues in steel–concrete mixed structures.

To overcome the adverse effects of shear strength in steel–concrete mixed structures, different techniques have been performed. One of these techniques involves the use of shear stud connectors, which serve to establish a strong connection between the steel girder and the concrete slab [5]. Typically, these connectors are welded to the steel girder's surface. Numerous types of shear connector types, including oscillating perfobond strips, waveform strips, headed studs, perfobond ribs, t-rib connectors, channel connectors, and non-welded connectors, have been used in composite beams [6]. Headed stud shear connectors are the most common type of shear connectors used in steel-concrete composite construction to transfer the longitudinal shear forces at the interface between steel and concrete. The behavior of headed stud shear connectors is explored by push-out tests. Stud shear connections are affected by many factors identified by previous research, with the main factors being shank diameter, height and tensile strength of studs, compressive strength and elastic modulus of concrete, and the direction of concrete casting [7]. Numerus research works have demonstrated that an increase in the shear strength, shear stiffness, and ductility was observed when a stud is added to in steel-concrete composite specimen [8-9]. Shim et al. [7] studied the design of shear connections in composite steel-concrete bridges using precast decks based on experimental push tests and a bridge model test. The results showed that uniform distribution of shear connectors is feasible due to their deformation capacity and load redistribution characteristics. They also observed that the ultimate strength of the shear connection is primarily influenced by the stud shank area. Similar findings were also observed in [10-11]. Xue et al. [12] examined how single-stud and multi-stud shear connections behave differently when subjected to static loads. The researchers tested ten push-out specimens, including four pairs with several studs in different configurations and one pair with a single stud measuring 22 mm in diameter by 200 mm in length. The findings demonstrated that the initial stiffness of single and multi-stud connections was comparable. However, using single-stud connections resulted in an increase in slip and ultimate strength of approximately 19% and 10%, respectively, compared to multi-stud configurations. Lin et al. [13] investigated the static shear behaviour of large-headed stud shear connectors implanted in ultra-high-performance concrete (UHPC) slabs. The pull-out experiments showed that the stud height significantly influenced the failure mode, tensile strength, and ultimate separation between the steel flange and the concrete slab. The stud connectors in the two innermost rows on either side of a transverse stiffener developed the tensile force in the studs as a result of transverse bending moments. Another study by Ovuoba and Prinz [14] investigated the fatigue capability of headed shear studs in composite bridge girders. The results indicated that the present AASHTO constant amplitude fatigue threshold (CAFL) for headed shear studs is overly conservative. Wang et al. [15] investigated the static behavior of large stud shear connections implanted in UHPC. The normal strength concrete (NC) slab specimen exhibited extensive splitting cracks, while the UHPC specimen with 30 mm studs showed no cracks, suggesting a good match between UHPC and large studs. An increase of around 15%, 45%, and 60% was observed in the shear strength, shear stiffness, and ductility of a stud with a 30 mm diameter compared to a stud with a 22 mm diameter, respectively. The authors also reported that the stud aspect ratio and concrete slab thickness had no significant effect on the behavior of the test specimens and that short-stud shear connections with an aspect ratio of 2.3 could achieve maximum strength in UHPC slabs. In recent years, Hu et al. [16] assessed the static shear performance of large-headed stud shear connections embedded in UHPC slabs. Nine specimens were examined to investigate the behaviour of single and group study arrangements. The performance of the tested beams was analysed with respect to cover thickness over the stud head, stud spacing in the transverse direction, and larger stud sizes. The obtained results indicated that using longer studs can increase the bending moment and deformation capacities. Also, they observed reducing the longitudinal stud spacing substantially enhanced the rigidity; however, it may lead to brittle failure of the concrete slab. The force exerted by a stud increases as its distance from the steel web increases, while its distance from the transverse stiffener decreases. Hence, the field-cast grouts used to fill the connection voids have rarely exhibited inferior durability. Finally, the intermittent full-depth pockets frequently specified for these composite connections lead to aesthetic, rideability, and durability issues in the finished bridge deck. For this reason, the use of UHPC in shear pockets has demonstrated considerable improvements in structural performance, especially in prefabricated composite beams and girders.

Using UHPC-filled pockets may result in significant benefits, including enhanced shear capacity and ductility, making them a viable option for modern construction techniques [17]. Nevertheless, an extensive amount of research has been carried out to assess the structural behavior of steel/UHPC composite beams with shear pockets. For example, Hu et al. [16] conducted research on the flexural performance of large-scale steel-UHPC composite beams. These beams are composed of a precast UHPC slab that is connected to the steel girder by large-headed stud clusters imbedded with shear pockets. The results have indicated that no splitting cracks appear in UHPC shear pockets, and no concrete crushing happens on the surface of the UHPC slab during the failure of beam specimens. UHPC and steel showed beneficial composite action, and the flexural performance of steel-UHPC composite beams is substantially enhanced. Additionally, the experimental tests reported by Zhang et al. [17] have shown that the shear resistance of the adhesive connection is significantly enhanced by the advanced properties of UHPC in comparison to conventional cementitious grouts. Huh et al. [8] examined the flexural behavior of the composite beams consisting of shear stud connectors placed in shear pockets, and precast UHPC slabs were attached to steel girders. The results provided recommendations for maximizing the design of composite beams that can lower construction costs

by utilizing precast UHPC slab joined by big stud clusters. Tests on composite beams revealed that the stud arrangement affected the flexural stiffness and strength. Compared to studs distributed regularly, clusters that were closely spaced initially had more rigidity. Furthermore, Huh et al. [18] indicated the incorporation of closely spaced studs in the shear pockets of the precast deck panels provides sufficient composite actions in the design of composite girders. In addition, the designs of shear studs (regularly spaced or clustered) have little influence on the composite's behavior. The composite action is unaffected by the absence of constraint to the shear studs due to the lack of reinforcing bars within the shear pockets.
It can be seen from the abovementioned research studies that very few experimental studies have investigated the structural behavior of composite steel-concrete beams with shear studs. More specifically, most of the reviewed research has primarily emphasized the structural performance of reinforced normal concrete (NC) rather than ultra-high-performance concrete (UHPC). Therefore, more experimental investigations are needed in this regard. In this study, the aim was to investigate the influence of shear studs on the structural behavior of UHPC beams made with varying distances and two different pocket distances.

2. Experimental work

In this work, four composite simply supported beams were tested and compared with a reference steel beam. Normal strength concrete (NC) slabs and UHPC pockets were designed and fabricated for studying the influence of shear stud alignment and number of shear pockets in the deck slab on the static behavior and shear strength of short-headed studs embedded in UHPC haunch between the steel girder and the deck slab. All the tested beams were made of steel -NC composite precast concrete slab. The composite action is ensured by using UHPC shear pockets and short-headed studs embedded in UHPC haunch. Table 1 shows the designation of the tested beams. For example, the first beam, denoted as “CG-2-30,” includes a NC slab with two shear pockets filled by UHPC and has short-headed studs spaced at 30 cm. The second one, denoted as “CG-3-30”, is similar to the first beam but with three pockets. The third one, denoted as “CGZ-2-30”, is composed of a two-shear pocket filled with UHPC and has studs with zigzag alignment . The fourth one, denoted as “CGZ-3-30”, is composed of a three-shear pockets filled by UHPC and has studs with zigzag alignment. All beams were subjected to static monotonic loading.

Table 1. *Identification of the tested beams.*

Beam designation	Beam details
R	Reference steel I beam
CG-2-30	Concrete composite – Two shear pockets – 30 cm shear stud spacing (alignment straight line)
CG-3-30	Concrete composite – Three shear pockets – 30 cm shear stud spacing (alignment straight line)
CGZ-2-30	Concrete composite – Two shear pockets – 30 cm shear stud spacing (alignment zigzag line)
CGZ-3-30	Concrete composite – Three shear pockets – 30 cm shear stud spacing (alignment zigzag line)

2.1 Geometrical properties and reinforcement details

Four NC concrete composite beam specimens consist of three major parts: the steel girder, the haunch, and the deck slab. The steel girders were attached to the deck slab by a haunch layer of UHPC, and UHPC shear lugs in the deck slab that are monolithic with the haunch and short-headed studs embedded in the haunch and does not pass through the shear pockets. The adhesive force between the different parts is also contributing to the composite action. The experimental program of this research comprised casting and testing four simply supported reinforced NC deck slabs composite with steel beams (W8X15). The deck slab dimensions are 250 mm in width, 75 mm in height, and 2000 mm in length. Figure 1 shows the details of the tested beams. The deck slabs were reinforced with two layers of steel mesh that has Ø8 mm steel bars, and the spacing between the longitudinal and transverse bars was 100 mm. The concrete cover from the top and bottom was 8 mm, whereas the concrete cover from the sides was 10 mm. The beam was designed according to AASHTO [19] and subjected to two-point loads at a distance of 300 mm up to failure. Further, for the deck slab, a wooden mould was made with three holes for the shear pockets to be poured after the deck slab to make the UHPC shear lugs monolithic with the haunch layer. The shear pockets were 100 X100 from the top and 90 mm X 90 mm from the bottom to prevent their separation from the deck slab as shown in Figure 2. The haunch layer was with dimensions of 50 mm height, 100 mm width, and 2000 mm length, placed on the upper flange of the steel girder. Figure 1presents details of the hang layer. The steel girder was the main part of specimens which was W8X15 with 200 mm in depth, 100 mm for flange width, 8 mm for flange thickness, 5 mm for web thickness, and 2000 mm for total length. The composite beams were divided into two groups according to the number of pockets and alignment of shear studs. The first group (CG-2-30, and CG-3-30) with beams that contain straight line of shear studs with spacing of 30 cm. In addition, it consists of two and three pockets for CG-2-30 and CG-3-30, respectively, as shown in Figure 3 and Table 1. The second group consists of two beams (CGZ-2-30, and CGZ-3-30) which consist of zigzag shear stud line, as shown in Figure 3 and Table 2.

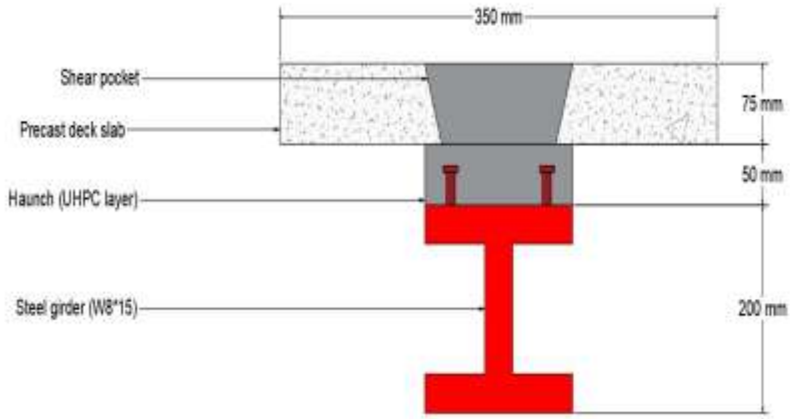

Figure 1. *Composite beam cross section.*

Figure 2. *Details of tested columns, a: reinforcement details, b: deck slab and pockets details*

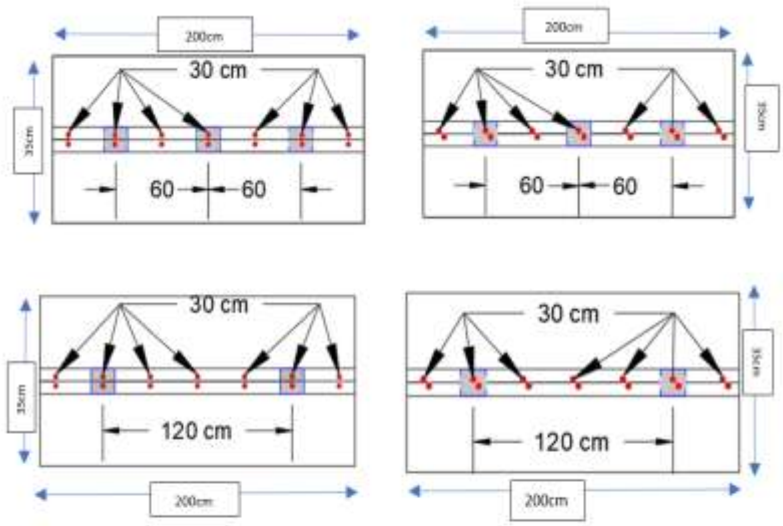

Figure 3. *Schematic diagram of tested beams*

Table 2. *Details of composite beams*

Beam ID	Number of shear pockets	Distance of shear studs (mm)	Alignment of shear studs
CG-2-30	2	300	Straight line
CG-2-30	3	300	Straight line
CGZ-2-30	2	300	Zigzag line
CGZ-2-30	3	300	Zigzag line

3. Materials

3.1 Binders

Ordinary Portland cement type I, sourced locally and compliant with the Iraqi Specification (IQS) [20], was utilized. The UHPC mix was created using silica fume that complies with ASTM C-1240 standards. [21]. The Sika Company provided it.

3.2Aggregate

In the study, two types of aggregates were utilized: fine aggregate with a maximum size of 4.75 mm and coarse aggregate with a maximum size of 20 mm (refer to Tables 3, 4, and 5 for details). All concrete mixtures utilized to cast conventional concrete and UHPC beams incorporated natural sand as the fine aggregate, while gravel—locally sourced crushed coarse aggregate—was used solely in the conventional concrete mixture as the coarse aggregate. Fine aggregate physical property test results are shown in Table 4. These tests were carried out at the Structural Laboratory of the Engineering Consulting Office at Al-Qadisiyah University's College of Engineering. The sieve analysis for this aggregate is shown in Table 5. All aggregates were utilized in saturated surface dry (S.S.D) conditions. Both coarse and fine aggregates meet the requirements of IQS [22].

Tables 3: Sieve analysis of fine aggregate.

Sieve size (mm)	% Passing by weight	Zone 2 limitation by IQS No. 45, 1984 [22]
10	100	100
4.75	96.4	100-90
2.36	85	100-75
1.18	72	90-55
0.6	51	59-35
0.3	27	30-8
0.15	3.6	10-0

Tables 4: Physical properties of the fine aggregate

Physical properties	Test result	Limit of No.45 /1984 [22]
Specific gravity	2.59	---
Sulphate content %	0.13	≤ 0.5
Fineness modulus	2.48	---

Tables 5: Sieve analysis of coarse aggregate

Sieve size (mm)	Cumulative passing %	limitation by IQS No. 45, 1984 [22]
19	100	100-95
13.2	60.8	-
9.5	32.2	60-30
4.75	0.6	10-0

3.3 Superplasticizer

In this research, a water-reducing admixture, ViscoCrete-180GS, served as the superplasticizer (SP). It was incorporated into the concrete mixture at a rate of 1% relative to the weight of cement. In addition, it complies with the standards of ASTM C-

494/C494M, types G and F [23]. The characteristics of the SP used are shown in Table 6.

Table 6: Technical data of ViscoCrete-180GS superplasticizer.

Property	Description
Composition	An aqueous solution of modified polycarboxylates
Packaging	1000 LTRs IBC 20 kg Pail
Appearance and color	Light brownish
Specific gravity	1.070+(0.02) g/cm^3
pH-Value	4-6

3.4 Steel bars

This study employed deformed steel bars with an 8 mm diameter for flexural reinforcement. The tensile strength of three specimens was tested following the guidelines of ASTM A615-05 [24]. The mechanical properties of these bars are shown in Table 7.

Table 7. *The mechanical properties of the tested steel bars.*

Property	Ø8
Yield stress (MPa)	449.18
Ultimate strength (MPa)	626.4
Elongation %	11.83

3.5 Steel Fibres

This study made use of micro-steel fibres (see Figure 4) for the production of high-strength concrete (HSC). With a length of 13 mm, these fibres have a diameter of 0.22 mm and an aspect ratio (L/D) of 59. They also demonstrate a considerable tensile strength of 2600 MPa..

Figure 4. *Micro-steel fibres used in producing HSC.*

3.6 Steel Girder

The steel girder used in this work is W8x15 with dimensions of 200 mm depth, 10 mm flange width, 8 mm flange thickness, and 5 mm web thickness. To test the mechanical properties of the steel beams, the Computer Numerical Control (CNC) machine was used to cut three tension dog bones (steel coupons) from the web and flange (Figure 5a). The yield stress of the used steel beams, as well as its ultimate strength are presented in Table 8. The dog bones conform to ASTM (A 370-05) [25]. For testing the dog bone samples, a universal testing machine was used (Figure 5b and c).

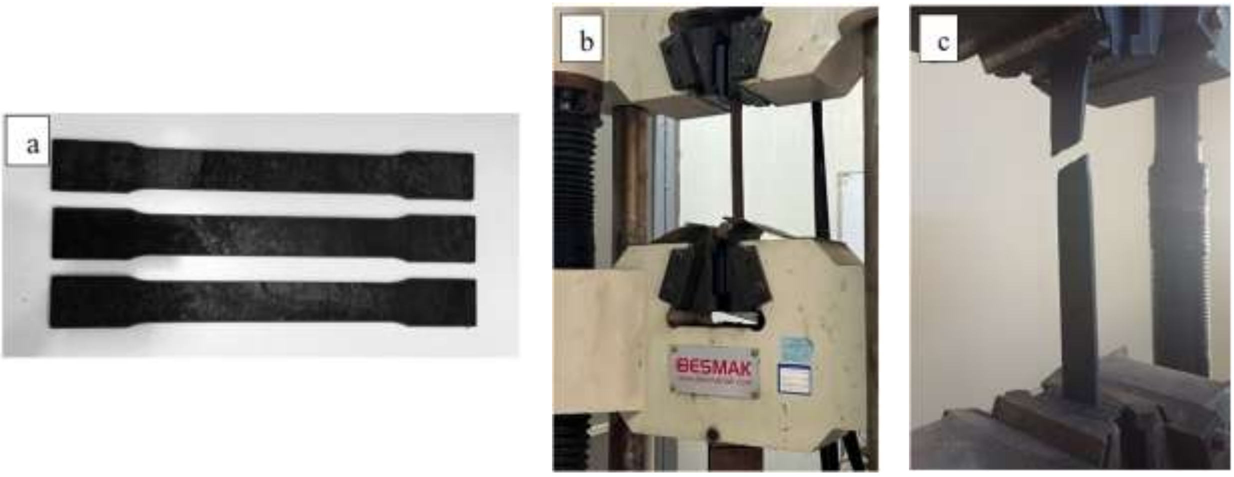

Figure 5. *Details of testing dog bones: (a) steel coupons, (b and c) tensile test machine.*

Table 8. *Properties of the used steel girder.*

Specimen No.	Yield stress (fy) MPa.	Ultimate stress (fu) MPa
Average of 3 samples	50	64.333

3.7 Stiffeners and shear connectors

A steel plate with a thickness of 4 mm was utilized as a stiffener for all simply supported beams tested. The stiffeners were welded on beam web on both sides under concentrated loads and at the supports (Figure 7). Three steel plate coupons were fabricated using a CNC machine in accordance with ASTM A370-05 requirements [25]. The mechanical properties of these specimens are shown in Table 9. This study utilized headed studs measuring 10 mm in length and 13 mm in diameter as shear connectors (see Figure 8a). The yield strength and ultimate tensile strength of the small-headed stud were 443.34 MPa and 695 MPa, respectively. As shown in Figure 8b, the studs were attached to the upper flange of the steel beams in two elongated rows, with a horizontal spacing of 75 mm between each pair (measured from center to center)..

Figure 7. *Details of the used stiffeners.*

Table 9. *The mechanical properties of the used stiffeners*

Specimen No.	Width mm	Thickness mm	Yield stress (fy) Mpa.	Ultimate stress (fu) MPa	Elongation %
Average of 3 samples	40	4	53.5	60.1	5.6

Figure 8. *Photographs of Headed Studs Shear Connectors Used.*

3.8 Mix proportion of NSC

Coarse aggregates, including both gravel and crushed stone, along with fine aggregates such as sand, in a saturated surface-dry condition were utilized in envisioning an NSC mixture with a water-to-cement proportion of 0.53. The constituents of the manufactured combinations were characterized dependent on the logical design technique expressed in the American Concrete Institute's blending proportions based on maximizing strength and workability (ACI 211.1-01), employing an intricate process relying on understanding the complicated interactions between aggregate, cement and water. Table 10 depicts the fixings of the amalgamation, listing the type and weight of each ingredient necessary to achieve the performance objectives.

3.9 Mix proportion of UHPC

Ultra-high-performance concrete (UHPC) mix, with a target compressive strength of 100 MPa, was prepared. The created UHPC mixturs was designed based on the mix proportioning method adopted in [27]. In the preparation of the UHPC mixture, one type of aggregate (fine aggregate) was used under saturated surface dry conditions with a maximum size of 600 micrometer. Additionally, micro-steel fibres with volume fraction of 1% were also used in this mix. Table 10 presents the quantity of ingredients used in the UHPC mix.

Table 10. *Constituent materials of the prepared concrete mixes, kg/m^3*

Mix type	w/c	Cement	Water	Silica fume	super-plasticizers%	Fine aggregate	Coarse aggregate	Steel fibre%
NSC	0.53	380	200	0	0	700	1100	0
UHPC	0.3	1000	300	100	800	1000	0	1

3.10 Composite beam specimens casting and curing

A prefabricated steel section was adhered to the upper face of the beam flange using an electric arc welding process. Concrete mixtures were prepared using a portable vertical mixer with a volumetric capacity of 0.2 cubic meters. Prior to pouring the concrete, a lubricant was applied to all interior surfaces of the forms to prevent adhesion. The deck slabs were then poured and their upper layers leveled and finished. With the exception of openings for shear connectors, an electrically powered vibrator was used to ensure thorough penetration of the fresh concrete into every tiny gap and void after casting the conventional deck with standard composite materials. The precast concrete deck slab was left to harden and cure for several days before being lifted and positioned above the girders within the haunch forms. Finally, the haunch and shear pockets were filled with an ultra-high performance concrete with a nominal compressive strength of 100 MPa through the openings intended for shear transfer, as shown in the designated figure. Samples of cubes, cylinders and prisms were cast from both mixtures to assess the mechanical qualities of the placed concretes. Thereafter, the specimens were stored under controlled laboratory conditions and covered to maintain humidity. After 21 days, the formwork was stripped away and the pieces wrapped in polypropylene sheeting to sustain a semi-regulated environment until achieving the designated age. The mixing, placing and curing of the test samples are depicted in the same indicated figure.

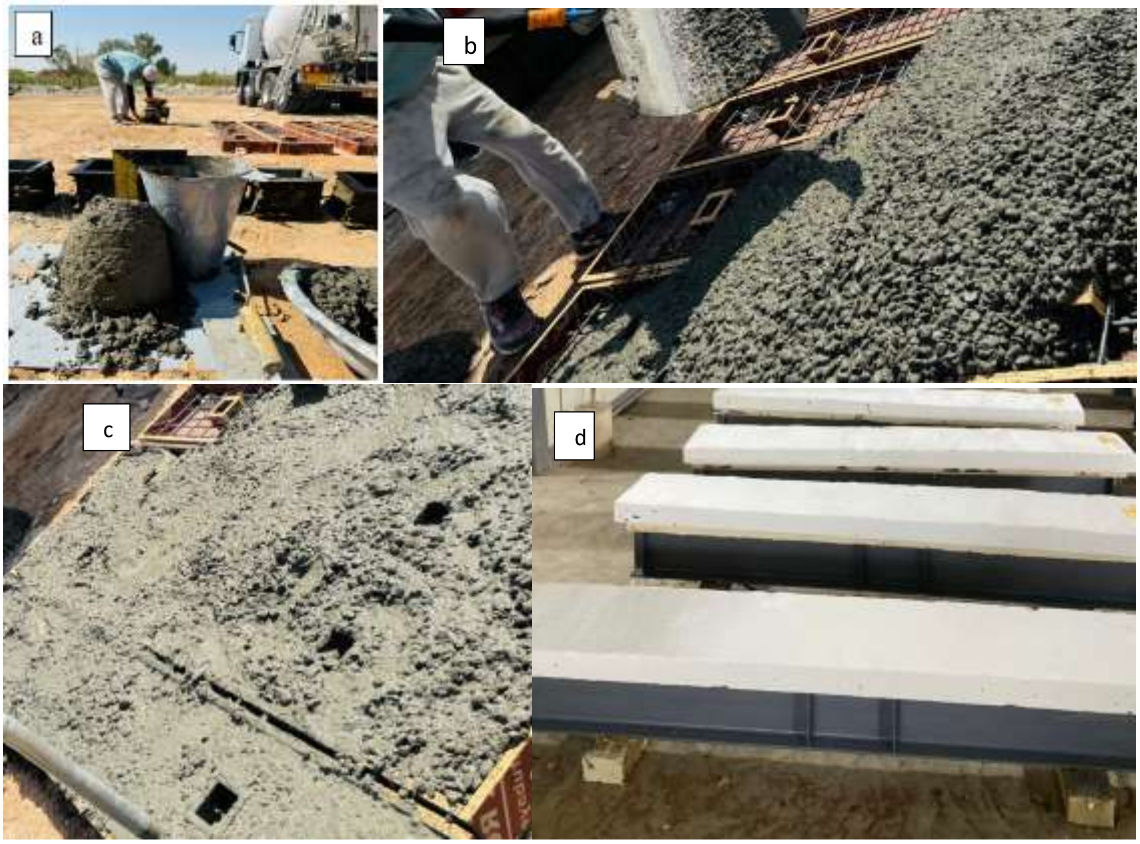

Figure 9. *Casting process of specimens :(a) slump flow, (b, c) casting deck slab concrete, and (d) completed specimen.*

3.11 Test Setup and Instrumentation

The composite beams were designed in accordance with AASHTO [19]. A universal testing instrument with a maximum capacity of 2000 kN was utilized for testing the beam specimens (Figure 10). The device is located in the Structural Laboratory of the Civil Engineering Department at Al-Qadisiyah University. As illustrated in Figure 11, the tested composite beams were painted two days prior to testing for easier observation of the developed and propagated cracks. Digital dial gauges with a maximum capacity of 50 mm were employed to measure the deflection at the mid-span of the beam as well as the sliding interaction between the concrete and steel components, which corresponds to the location of the maximum flexural moment due to the applied load.

Figure 10. *The used hydraulic testing machine*

4. Results and discussion

Four reinforced concrete composite beams made with normal and UHPC slabs were prepared to investigate their structural behavior and compared with a reference steel girder. Two beams, which were made of two shear pockets strengthened by hex head bolts aligned in straight and Zigzag lines, were tested until failure, while the others were made from three shear pockets. Table 11 summarizes the experimental test results for the composite beam specimens, including their ultimate capacity, failure load, and failure mode. In addition, Table 12 presents the first visible flexural cracks load, and ultimate failure load for tested beams. The following sections discuss and evaluate the results along with the load-displacement curves.

Table 11. *Experimental results for the tested composite beams.*

No.	Beam designation	No. of shear pockets	Alignment of shear studs	Ultimate capacity (kN)	Failure load increase over Control beam*	Δ_{max} (mm)	Ratio relative to the control beam*	Failure mode
1	R	--	--	169	--	14.39	--	Local buckling in the top flange
2	CG-2-30	2	Straight	250	+47.93%	18.41	+27.94%	Debonding between deck slab and the
3	CG-3-30	3	Straight	260	+53.85%	14.82	+2.99%	Debonding between deck slab and the
4	CGZ-2-30	2	Zigzag	270	+59.76%	16.81	+16.82%	Debonding between deck slab and the
5	CGZ-3-30	3	Zigzag	277	+63.91%	16.95	+17.79%	Debonding between deck slab and the

*This is the ratio of the ultimate load of beams relative to the control beam, (+) means increase (%) in the above properties with respect to the reference beam, (-) means decrease (%) in the above properties.

Table 12. *Cracking loads for tested beams.*

Specimen ID	First crack Load on deck slab Pcr (kN)	Ultimate load Pu (kN)	$\frac{Pcr}{Pu}$ *100 (%)
CG-2-30	80	250	32
CG-3-30	85	260	33
CGZ-2-30	70	270	26
CGZ-3-30	90	277	32.49

4.1 Effect of shear pockets numbers for straight bolts line

a. Load-mid span deflection response

Analysing the relationship between mid-span deflection and applied load for each beam was part of the testing method. The load deflection behaviour is shown in Figure 11 for beams with straight bolt line. This group of comparison includes three beams designated as R, CG-2-30, and CG-3-30, where the composite beams have the same spacing of studs (30 cm) but different numbers of shear pockets, as shown in Table 11. Table 11 and Figure 11 demonstrate that the control beam maintains its linear behaviour up to yielding that occurred in the bottom flange and local buckling that occurred in the top flange when the beam failed. Similar linear but stiffer behaviour was observed in the composite beams until the first crack of the deck slab. After that, the load-deflection curve becomes nonlinear, leading to a decrease in the specimen's stiffness due to the concrete cracks and yielding of the steel girder. When comparing the load-displacement curves of tested beams with different numbers of shear pockets, the maximum load-carrying capacity for the R, CG-2-30, and CG-3-30 beams is 169 kN, 250 kN, and 260 kN, respectively. In addition, the mid-span displacements for tested beams were 14.39 mm, 18.41 mm, and 14.82 mm, respectively. As a result, composite beams presented an increase of approximately 47.93% and 53.85% in ultimate failure load compared to reference beam, respectively. Regarding the composite UHPC beams with shear pockets strengthened by straight lines of stud bolts, it was obviously observed that these beams exhibited a higher stiffness than that of unstrengthened beam (reference beam). The increase was about 53.85% for three shear pocket beam compared with a two pocket beam; see Table 11. It can be noted that the failure modes of the two composite beams are obviously similar. At the failure point of the beams CG-2-30 and CG-3-30, a debonding between the deck slab and the haunch layer failure mode occurred. Differently, the steel girder yielded, and no crushing of UHPC was observed at the failure point of the tested beams except that at the interface of the deck slab and the haunch.

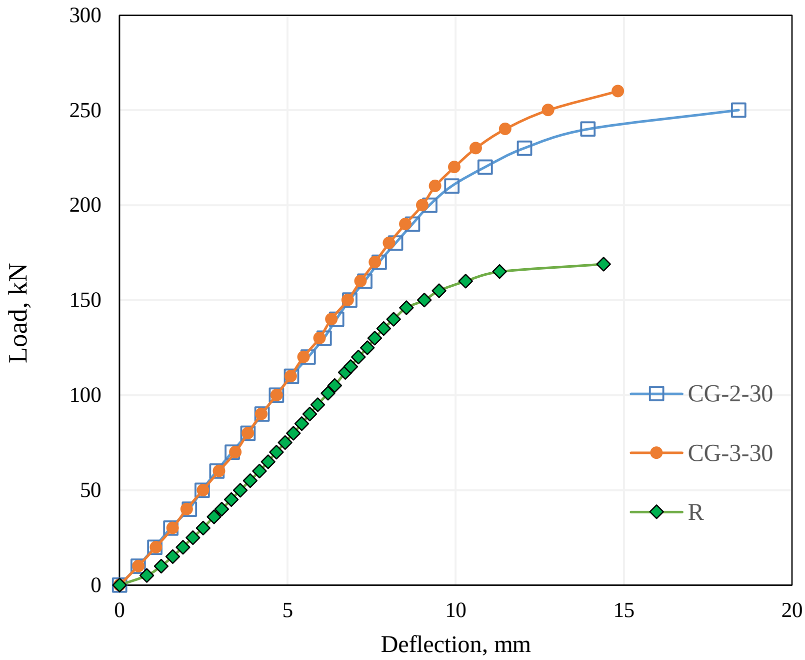

Figure 11. *Load–deflection response for composite beams with straight-line studs bolts.*

b. Crack Patterns and Failure Modes

Figure 12 and Table 12 show the crack patterns and failure modes of the composite beams with studs arranged at straight lines with a variety of numbers of shear pockets. For CG-2-30 beam, visual cracks appeared at the top surface of the NC slab, close to the loading point at a load of 80 kN (i.e., 32% of the ultimate load). As the load increased, vertical cracks appeared on the side surface of the NC slab and the UHPC shear pocket. At a load of 250 kN, the NC slab at the loading point was crushed. The cracking pattern of the beam CG-3-30 at failure is shown in Figure 12. The cracks started to appear on the side and bottom of the UHPC haunch at a load of 30 kN. With a further increment of the applied load, more cracks appeared in the UHPC haunch, and the steel girders were failed, yielding an extension of the cracks. It can be seen from Figure 12 that most of the cracks of the tested beams are distributed on the shear span and especially pure bending section, with the cracks in the deck slab of CG-2-30 beam started to appear earlier due to the huge distance between the shear pockets. However, the number of cracks in the haunch for CG-3-30 beam is greater but thinner than that of CG-2-30 beam. When the specimen failure occurred, the crack width of all tested beams was tiny, indicating that the bridging effect of steel fibers restrains the propagation of cracks. Moreover, no splitting cracks were found in the UHPC shear pocket for all beams at the failure load. All beams failed in debonding between the deck slab and the haunch layer.

Figure 12. *Crack patterns and failure mode of the composite beams strengthened with straight-line studs.*

4.2 Effect of number shear pockets for zigzag bolts line

a. Load-mid span deflection response

A comparison of load-displacement curves is shown in Figure 13 of composite beams connected by zigzag lines of shear studs that have different numbers of shear pockets. This group of comparison contains three beams (R, CGZ-2-30, and CGZ-3-30) and the composite beams have similar stud spacing (30 cm) but their alignments are in zigzag lines, as indicated in Table 11. Only the numbers of shear pockets are different in this group. Beam R is a reference beam in this group, whereas beam CGZ-2-30 was cast to investigate the effect of number of shear pockets with zigzag-line alignment, and beam CGZ-3-30 was with three shear pockets and zigzag-line alignment. Figure 13 and Table 11 demonstrate that the CGZ-2-30 and CGZ-3-30 specimens have maximum load capacities of 270 kN and 277 kN, respectively, with corresponding mid-span displacements of 16.81 mm and 16.95 mm. The increased number of shear pockets improved the load and stiffness of the tested beam, as shown in Figure 13. The effect of composite action technique in improving the ultimate failure load showed an increase about 59.76% and 63.91%, respectively, when compared to the reference beam. On the other hand, the maximum load capacity of the CGZ-3-30 beams is about 2.59% higher than the CGZ-2-30 beam. Obviously, the use of more shear pockets in the composite action significantly increased the cracking load in both of the composite beams that were evaluated.

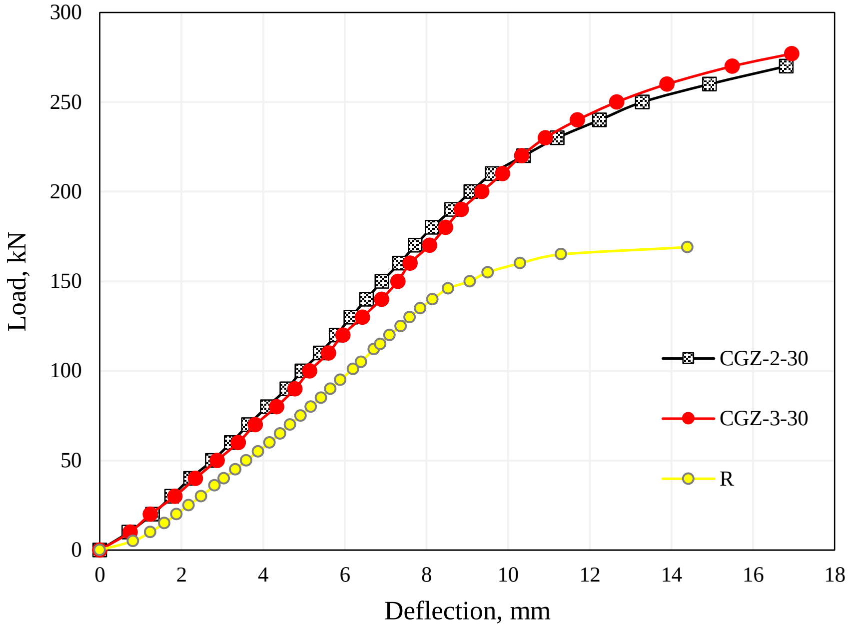

***Figure 13**. Load–deflection response for composite beams with zigzag-line studs.*

b. Crack Patterns and Failure Modes

Figure 14 shows the crack patterns observed for the composite beams with studs arranged at zigzag lines at failure. Initially, the first visible cracks occurred in beam specimens CGZ-2-30 and CGZ-3-30 under loads of 70 kN and 90 kN, respectively (see Table 12). As the load progressed, the cracks propagated toward the load points. The specimens carried a peak shear load of 270 kN, and 277 kN for two and three shear pockets, respectively. At this load, the cracks began to widen in the UHPC haunch and NC slab. Additionally, the steel girder web reached yielding. No damage was observed within the UHPC connection or in the steel elements (i.e., rebar or studs). The CGZ-3-30 specimen began to show increasing diagonal shear cracks movement along the slab towards the applied point loads. Regardless, the overall performance of the composite specimen is good. All beams failed in debonding between the deck slab and the haunch layer. Thus, it is recommended to improve the strength of haunch and shear pocket material and increase the pocket area to achieve full composite action. In addition, An effective composite action was developed between shear studs and the haunch layer.

***Figure 14.** Crack patterns and failure mode of the composite beams strengthened with zigzag-line studs' bolts.*

3.2 Effect of stud alignment on two shear pocket beams

a. Load-mid span deflection response

The effect of the stud alignment line on load-deflection for composite beams with two shear pockets is shown in Figure 15. This comparison group includes three beams designated as R, CG-2-30, and CGZ-2-30, which were similar in stud spacing and included two shear pockets, as shown in Table 11. Beam R was the reference beam of this group. Beam CG-2-30 was cast with two shear pockets, 30 cm stud spacing, and studs aligned in a straight line, while beam CGZ-3-30 was made of three shear pockets, 30 cm stud spacing, and studs aligned in a zigzag line. It is obvious that the maximum deflection values in these beams were higher than those in the reference beam, which varied from 16.81 mm to 18.41 mm. It is evident that the addition of shear studs in zigzag lines improved the capacity of the beam compared with the beam with straight line studs due to the better proximity that this geometry creates with the shear pockets which helps better transfer the load.

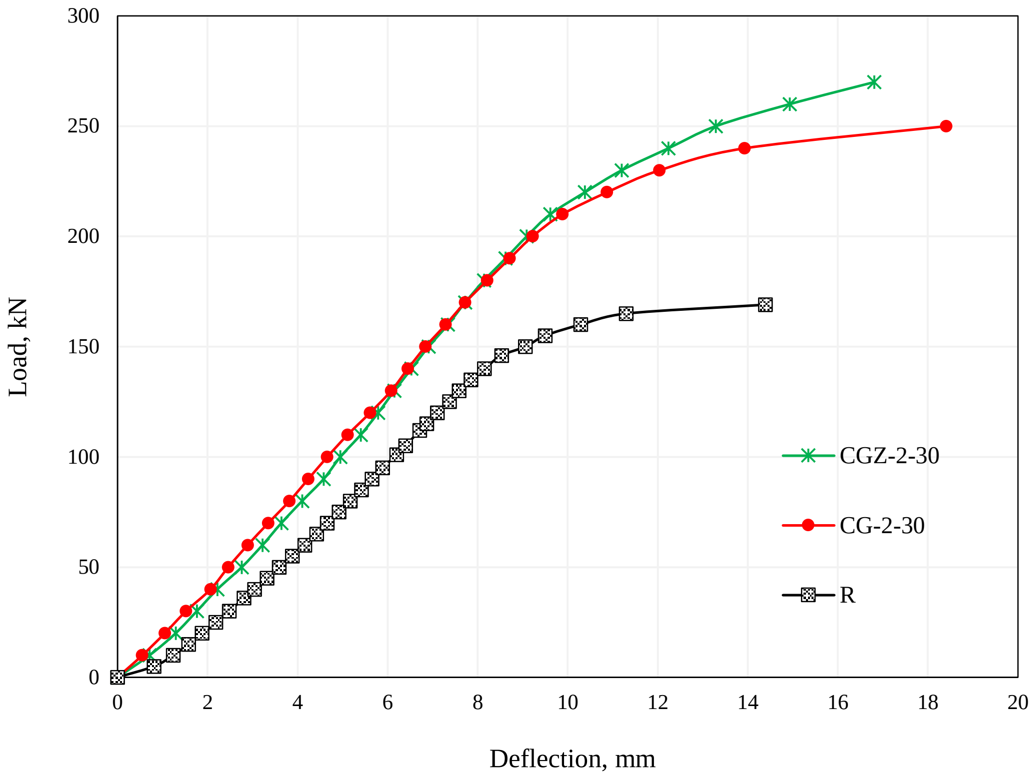

Figure 15. *Load–deflection response for composite beams with two shear pockets.*

b. Crack Patterns and Failure Modes

Figure 16 and Table 12 display the cracking load, crack patterns, and failure modes of composite beams strengthened by shear studs with two shear pockets and different alignment lines. Visible cracks were observed only at the top of the slab. Table 12 shows that the first flexural cracks of the beam specimens CG-2-30 and CGZ-3-30, which were reinforced with two shear pockets, appeared at the loads of 80 kN and 70 kN, respectively. Further increasing the applied load, numerous diagonal cracks developed along the full length of the tested beams in the slab and UHPC haunch layer parts, while the yielding failure occurred in the steel girder. The failure pattern of all tested beams and the mode of failure were deponding on the deck slab and the haunch layer failures, as shown in Figure 16. It can be concluded that an effective composite action was developed between the deck slab and the steel girder in all tested beams; composite behaviour was not affected by stud configuration, increased girder stiffness, or absence of restraining bars in the shear pockets.

Figure 16. *Crack patterns and failure mode of the composite beams strengthened with different alignment-line studs' bolts (two shear pockets).*

3.3 Effect of stud alignment on three shear pocket beams

a. Load-mid span deflection response

Figures 17 and Table 11 compare the load-deflection relationships of the control and strengthened RC composite beams at three shear pockets of the studs. It can be seen from these figures that when the zigzag-line alignment of bolts in hunch layers (bolts spaced 30 cm), as shown in Figure 17, the maximum load capacity of the strengthened beams was considerably increased. This effect can be clearly seen in Table 11, which shows that the maximum load capacity of the CG-3-0 and CGZ-3-30 specimens is 260 kN and 277 kN, which is about 53.85% and 63.91% higher than that of the control beams, respectively, with a corresponding mid-span displacement of 14.82 mm and 16.95 mm. The ultimate load capacity of the strengthened composite beams was greatly increased when three shear pockets were utilised instead of two shear pockets, as well as this improvement was observed when zigzag-line alignment instead of straight line for hunch layers. Thus, the failure mode for all tested beams was deponding between the deck slab and the haunch layer. On the other hand, the addition of shear studs in hunch layers improved the stiffness of the tested beams, as shown in Figure 17. Furthermore, it is expanded the area under the load-deflection curve, hence increasing energy absorption capacity. In addition, the shear studs improve the toughness, crack control, and overall capacity of composite beams.

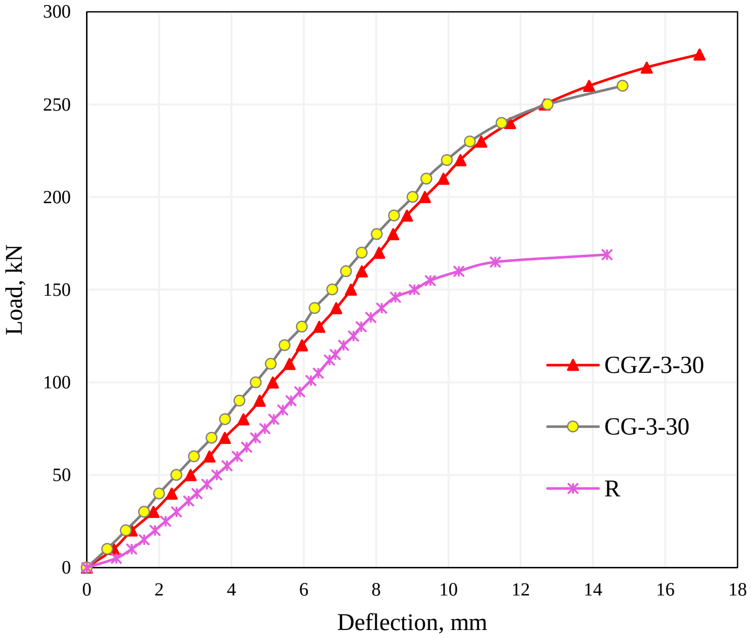

Figure 17. *Load–deflection response for composite beams with three shear pockets.*

b. Crack Patterns and Failure Modes

Figures 18 and Table 12 illustrate the crack patterns, the occurrence of the first flexural crack, and the failure modes of both the control and strengthened composite beams, which utilized various bolt alignments in the hunch layer embedded within the concrete slab and incorporated three shear pockets.Test results indicate that the first visible flexural crack appeared at loads of 80 kN for the strengthened beam CG-3-30 and at 90 kN for CGZ-3-30, despite both beams having identical bolt spacing and shear pocket counts. Generally, Table 12 reveals that using stud bolts in a zigzag alignment in the hunch layer effectively delays the appearance of the initial crack.Table 11 shows that all strengthened beams experienced de-bonding within the concrete layers as their failure mode. Figure 6 depicts the failure behavior of the composite beam group, highlighting that the primary fracture reached the top components of the concrete slab, occurring at the bond between the deck slab and the hunch layer.The novel UHPC connections successfully resisted all applied loads throughout the testing program, with no damage observed in the UHPC composite connection or the adjacent steel connectors. During the final testing phase, the horizontal shear stress in the field-cast UHPC haunch exceeded the capacity of the composite connection's shear plane. At this point, yielding in the web of the steel girder began, while the hunch layers and slab components were subjected to a combination of horizontal and vertical shear stresses, ultimately leading to failure through de-bonding.

Figure 18. *Crack patterns and failure mode of the composite beams strengthened with different alignment-line studs' bolts (three shear pockets).*

5. Conclusions

An experimental investigation into the response of a precast composite concrete slab connected with a steel girder using a UHPC haunch and shear lugs under static loads was presented. For this purpose, five specimens subjected to different loads were considered. Two variables were considered in the experimental tests, including the numbers of shear pockets and the alignments of bolt lines. The following conclusions can be drawn from the present study:

1. It was observed that the mode of failure of composite deck slabs exhibited flexural failure, cracks were formed in the compression zone under the point load and propagated to the surrounding concrete, and yielding occurred in the steel beam. As the applied force increased, the cracks developed more, forming longitudinal and diagonal cracks.
2. The number of shear pockets significantly influences the behavior of composite beams, where it seems that the specimens with three shear pockets have better performance than those with two pockets by 2%, the presence of three shear pockets might provide better balance or more strength and stability, enhancing overall performance.
3. The zigzag-line bolts performed better than the straight-line bolts in terms of loading capacity.

Author Statements:

- **Ethical approval:** The conducted research is not related to either human or animal use.
- **Conflict of interest:** The authors declare that they have no known competing financial interests or personal relationships that could have appeared to influence the work reported in this paper
- **Acknowledgement:** The authors declare that they have nobody or no-company to acknowledge.
- **Author contributions:** The authors declare that they have equal right on this paper.
- **Funding information:** The authors declare that there is no funding to be acknowledged.
- **Data availability statement:** The data that support the findings of this study are available on request from the corresponding author. The data are not publicly available due to privacy or ethical restrictions.

References

[1] Shamass, R., & Cashell, K. A. (2017). Behaviour of composite beams made using high strength steel. *Structures, 12*, 88–101.

[2] Mansour, F. R., Bakar, S. A., Ibrahim, I. S., Marsono, A. K., & Marabi, B. (2015). Flexural performance of a precast concrete slab with steel fiber concrete topping. *Construction and Building Materials, 75*, 112–120.

[3] Khadhair, A. Y., & Izzet, A. F. (2024). Behavior of reinforced concrete beams with vertically penetrated holes across the cross-section depth. *Engineering, Technology & Applied Science Research, 14*(3), 14301–14307.

[4] Ali, D. Y., & Mahmood, R. A. (2024). Influence of slenderness ratio and section geometry on the behavior of steel braced frames. *Engineering, Technology & Applied Science Research, 14*(3), 14282–14286.

[5] De Lima, A. D., Sales, M. W. R., De Paulo, S. M., & De Cresce El, A. L. H. (2016). Headed steel stud connectors for composite steel beams with precast hollow-core slabs with structural topping. *Engineering Structures, 107*, 135–150.

[6] Ali, S. N. H., Ramli Sulong, M. S., & M. S. (2012). Investigation of channel shear connectors for composite concrete and steel T-beam. *International Journal of the Physical Sciences, 7*(11). https://doi.org/10.5897/ijps11.1604

[7] Chang-Su, S., Pil-Goo, L., Dong-Wook, K., & Chul-Hun, C. (2011). Effects of group arrangement on the ultimate strength of stud shear connection. In *International Conference on Composite Construction in Steel and Concrete VI*, *9*(23).

[8] Huh, B., Lam, C., & Tharmabala, B. (2015). Effect of shear stud clusters in composite girder bridge design. *Canadian Journal of Civil Engineering, 42*(4), 259–272.

[9] Hu, Y., Yin, H., Ding, X., Li, S., & Wang, J. Q. (2020). Shear behavior of large stud shear connectors embedded in ultra-high-performance concrete. *Advances in Structural Engineering, 23*(16), 3401–3414.

[10] Lam, D., & El-Lobody, E. (2005). Behavior of headed stud shear connectors in composite beam. *Journal of Structural Engineering, 131*(1), 96–107.

[11] Hanswille, G., Porsch, M., & Ustundag, C. (2007). Resistance of headed studs subjected to fatigue loading: Part I: Experimental study. *Journal of Constructional Steel Research, 63*(4), 475–484.

[12] Xue, D., Liu, Y., Yu, Z., & He, J. (2012). Static behavior of multi-stud shear connectors for steel-concrete composite bridge. *Journal of Constructional Steel Research, 74*, 1–7.

[13] Lin, Z., Liu, Y., & Roeder, C. W. (2016). Behavior of stud connections between concrete slabs and steel girders under transverse bending moment. *Engineering Structures*, *117*, 130–144.
[14] Ovuoba, B., & Prinz, G. S. (2016). Fatigue capacity of headed shear studs in composite bridge girders. *Journal of Bridge Engineering*, *21*(12), 4016094.
[15] Wang, J., Qi, J., Tong, T., Xu, Q., & Xiu, H. (2019). Static behavior of large stud shear connectors in steel-UHPC composite structures. *Engineering Structures*, *178*, 534–542.
[16] Hu, Y., Meloni, M., Cheng, Z., Wang, J., & Xiu, H. (2020). Flexural performance of steel-UHPC composite beams with shear pockets. *Structures*, *27*, 570–582.
[17] Zhang, Y., Zhang, H., Tang, M., & Hou, Z. (2021). An enhanced UHPC-grout shear connection for steel-concrete composite bridges with precast decks. *Advances in Civil Engineering*, *2021*, Article ID 5595174. https://doi.org/10.1155/2021/5595174
[18] Huh, B., Lam, C., & Tharmabala, B. (2015). Effect of shear stud clusters in composite girder bridge design. *Canadian Journal of Civil Engineering*, *42*(4), 259–272.
[19] American Association of State Highway and Transportation Officials. (1993). *AASHTO guide for design of pavement structure*. Washington, D. C.: AASHTO.
[20] Iraqi Organization of Standards. (1984). *IQS 5/1984: Specification for Portland cement*. Baghdad, Iraq.
[21] ASTM. (2004). *ASTM C1240-04: Standard specification for the use of silica fume as a mineral admixture in hydraulic cement concrete, mortar and grout*. Vol. 4.2.
[22] Iraqi Organization of Standards. (1984). *IQS 45/1984: Specification for aggregate*. Baghdad, Iraq.
[23] ASTM. (2013). *ASTM C494/C494M-13: Standard specification for chemical admixtures for concrete*. Annual Book of ASTM Standards.
[24] ASTM. (2009). *ASTM A615/A615M-09b: Standard specification for deformed and plain carbon-steel bars for concrete reinforcement*.
[25] ASTM. (2009). *ASTM A370: Standard test methods and definitions for mechanical testing of steel products*. West Conshohocken, PA: ASTM International.
[26] American Concrete Institute. (2002). *ACI 211.1-91: Standard practice for selecting proportions for normal, heavyweight, and mass concrete* (Reapproved 2002).
[27] Kinaine, A. F. (2023). *Development of joint-less rigid pavement using ultra-high performance concrete link slab* (Master's thesis). Roads and Transport Engineering.